http://dx.doi.org/10.5012/bkcs.2013.34.5.1435

Effect of Carbon Matrix on Electrochemical Performance of Si/C Composites for Use in Anodes of Lithium Secondary Batteries

Eun Hee Lee, Bo Ock Jeong, Seong Hun Jeong, Tae Jeong Kim, Yong Shin Kim,† and Yongju Jung*

Department of Chemical Engineering, Korea University of Technology and Education (KOREATECH), Cheonan 330-708, Korea
**E-mail: yjung@koreatech.ac.kr*
†Department of Applied Chemistry and Graduate School of Bio-Nano Technology, Hanyang University, Ansan 426-791, Korea
Received December 14, 2012, Accepted February 14, 2013

To investigate the influence of the carbon matrix on the electrochemical performance of Si/C composites, four types of Si/C composites were prepared using graphite, petroleum coke, pitch and sucrose as carbon precursors. A ball mill was used to prepare Si/C blends from graphite and petroleum coke, whereas a dispersion technique was used to fabricate Si/C composites where Si was embedded in disordered carbon matrix derived from pitch or sucrose. The Si/pitch-based carbon composite showed superior Si utilization (96% in the first cycle) and excellent cycle retention (70% after 40 cycles), which was attributed to the effective encapsulation of Si and the buffering effect of the surrounding carbon matrix on the silicon particles.

Key Words : Li secondary battery, Si/C composite, Carbon matrix, Silicon

Introduction

As a result of technological breakthroughs over the past 20 years, lithium ion batteries have been widely used as a power source for the majority of portable electronic devices. In practice, lithium battery technologies led to the revolutionary development of wireless IT devices and the rapid expansion of the electric vehicle market. At present, however, the lithium battery industry faces a serious challenge due to limitations on energy density.[1] Recent advances in nanotechnology have presented new opportunities to resolve this bottleneck.[2] Many candidate materials have been developed to replace current graphite materials for use in anodes for the next generation of lithium batteries.[3-5] Lithium storage materials have attracted much attention due to their large theoretical capacities.[4-6] However, these materials have not been used for practical applications in lithium batteries due to their poor cycle properties and swelling phenomena, which originate primarily from volume expansion during charge/discharge cycles.[7,8] To address these issues, lithium storage material-based carbon composites have been developed. Silicon-based carbon composites have been studied intensively.[9-18] Various approaches to make these materials have included simple blending of silicon and carbon, introducing nano-sized silicon particles into a matrix and coating silicon or silicon composites with conductive materials.[9-18] In case of Si/C nanocomposites, it has been widely accepted that silicon nanoparticles should be evenly dispersed through the carbon matrix to mitigate the distortion or fragmentation of the composite materials, which is caused by the volume expansion of the silicon particles.[19,20] A number of Si/C composites with high capacity and excellent cycle life have been demonstrated. Most researchers have made Si/C composites with a single type of carbon or carbon precursor and evaluated their electrochemical properties. Thus far, a comprehensive overview of the influence of carbon type on the electrochemical performance of Si/C composites has not been presented. In this work, four types of Si/C composites were prepared using graphite (a crystalline form of carbon), petroleum coke (a soft carbon precursor), pitch (a soft carbon precursor) and sucrose (a hard carbon precursor) (Fig. 1). The preparation technique for each Si/C composite depends on the carbon precursor. Solid samples of silicon and graphite (or petroleum coke) were blended by ball milling, whereas silicon was embedded into carbon matrix derived from pitch and sucrose. Except for the Si/graphite composite, the Si/C composites were made by carbonizing the Si/carbon precursor composites. Finally, the electrodes were fabricated from the silicon/carbon composites, binder and

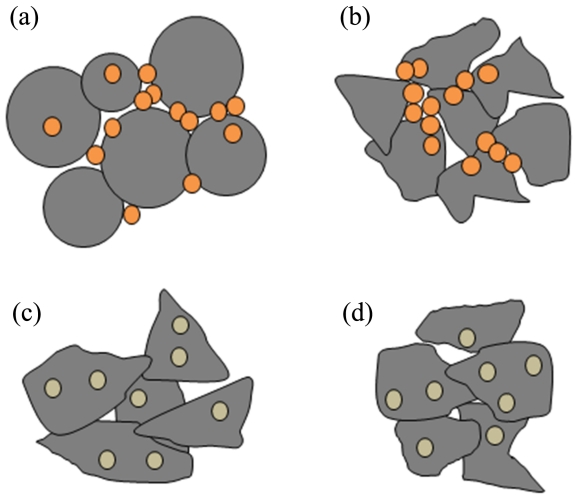

Figure 1. Schematic images of Si/C composites: (a) Si/graphite blended composite; (b) Si/petroleum coke-based carbon blended composite; (c) Si-embedded soft carbon composite; and (d) Si-embedded hard carbon composite.

carbon black, and their electrochemical properties were examined in coin-type cells.

Experimental

Preparation and Characterization of the Si/C Composites. First, silicon nanopowder (0.5 g, D_{50} = 50 nm, Cheorwon Plasma Research Institute, Korea) was dispersed uniformly in ethanol (50 mL) by ultrasonication. The Si solution was added to another ethanol solution (20 mL) in which graphite powder (4.5 g, mesocarbon microbeads, MCMB) was dispersed by ball milling for 6 h. The resulting colloidal solution was blended until it was homogeneous by ball milling for 12 h. The mixture was filtered and dried under vacuum at 120 °C overnight to obtain Si/graphite blended composites (Si-GB). Second, Si/coke blends were prepared from 0.5 g silicon and 4.5 g petroleum coke (GS Caltex, Korea) by the blending method (above) and carbonized at 900 °C under argon for 3 h to make Si/petroleum coke-based carbon blended composites (Si-PCB). Third, pitch powder (5.14 g, Posco Chemtech, Korea), a carbon precursor, was dissolved in 100 mL tetrahydrofuran (THF) by ultrasonication. Another solution, in which 0.4 g silicon nanopowder was predispersed in 50 mL THF by ultrasonication, was added to the pitch solution and agitated at room termperature until the mixture dried. The mixture of pitch and silicon was carbonized at 900 °C under argon for 3 h to make composite materials of Si nanoparticles embedded in soft carbon (SiE-SC). Lastly, 0.5 g silicon nanopowder was uniformly dispersed in 150 mL of distilled water by ultrasonication. The Si solution was added in a solution of 12.5 g sucrose and 0.8 mL H_2SO_4. The mixture solution was dried at 110 °C for 6 h, at 160 °C for additional 6 h and carbonized at 900 °C under argon for 3 h to make composites of Si nanoparticles embedded into hard carbon (SiE-HC). The proportion of Si and the three types of carbon precursors (petroleum coke, pitch, sucrose) was determined by trial and error to make Si/C composites with similar ranges of Si content. Three disordered carbons were prepared from the three types of carbon precursors with the same method as used in the synthesis of each Si/C composite except for adding Si nanopowders. The Si/C composites were evaluated by thermal gravimetric analysis (TGA) at a heating rate of 10 °C/min (Perkin Elmer, TGA4000). X-ray Diffraction (XRD) patterns were recorded with a Rigaku Ru200B diffractometer using Cu K_α radiation. Scanning electron microscope (SEM) images were taken using a JEOL JSM-7500F microscope operated at 10 kV.

Electrochemical Evaluation of the Si/C Composites. Electrodes were prepared from mixtures of 80 wt % Si/C composite or carbon as an active material, 5 wt % carbon black (Super-P) as a conducing agent and 15 wt % polyvinylidene difluoride (PVDF) as a binder. The three materials were agitated in *N*-methyl-2-pyrrolidone (NMP) solvent to make a slurry, which was coated on copper foil. The coated electrodes were dried in a convection oven at 120 °C for 1 h, pressed, dried at 130 °C under vacuum for 12 h and assembled into cells. The cell electrolyte was 1 M $LiPF_6$ in ethylene carbonate (EC)/ethyl methyl carbonate (EMC) (3:7, v/v, Panax Etec) with 2 wt % fluoroethylene carbonate (FEC) as an additive. Coin-type half-cells (CR2016) were assembled with a lithium metal foil as a counter electrode in an argon-filled glove box. Charge/discharge tests of the cells were conducted in the voltage range between 0.005 and 1.5 V *vs*. Li/Li^+ at 25 °C. A constant current-constant voltage (CC-CV) mode was used for the discharge tests, whereas a constant current (CC) mode was used for the charge test. The CC-CV tests were carried out in two steps: 1) discharge to 5 mV under a constant current; and 2) subsequent discharge at 5 mV until the current reaches the cut-off value of 0.01 C (1 C = 372 mAh/g). During the first two cycles, the charge/discharge curves were obtained at a fixed rate of 0.1 C. Subsequently, the rates were 0.2 C during the charge/discharge cycle tests.

Results and Discussion

The XRD pattern of Si-GB contains diffraction peaks for crystalline phases of graphite and silicon, whereas the XRD patterns of the other Si/C composites contain only the Si crystalline peaks (Fig. 2). The (002) peak at approximately 26, which arises from the stacking of carbon layers, was very broad in Si-PCB and SiE-SC, and negligible in SiE-HC, indicating the formation of highly disordered carbons.[21] It is notable that other impurity peaks due to SiO_2 and SiC were not observed.

The SEM images of Si-GB and Si-PCB clearly show that silicon nanoparticles were well dispersed on the surfaces of the carbon particles, although some silicon particles were aggregated (Fig. 3). However, very few silicon particles were observed on the carbon surfaces in SiE-SC and SiE-HC, indicating that the Si particles were embedded in the carbon as a consequence of the fabrication technique.

To determine the silicon content in the Si/C composites, TGA analysis was performed under an ambient atmosphere. The samples were dried completely at 200 °C, cooled to 80 °C and heated from 80 to 900 °C at a rate of 10 °C/min.

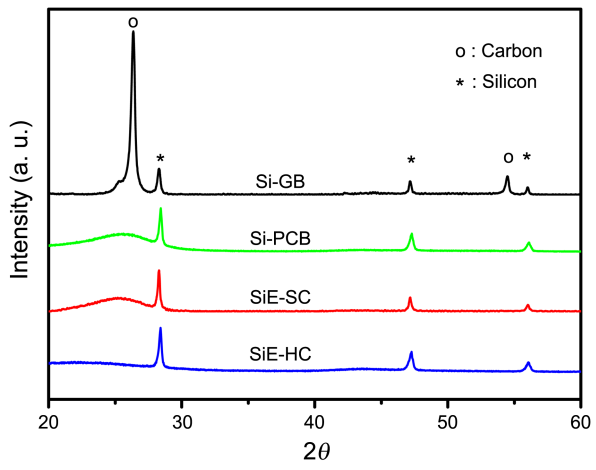

Figure 2. XRD patterns of Si/C composites.

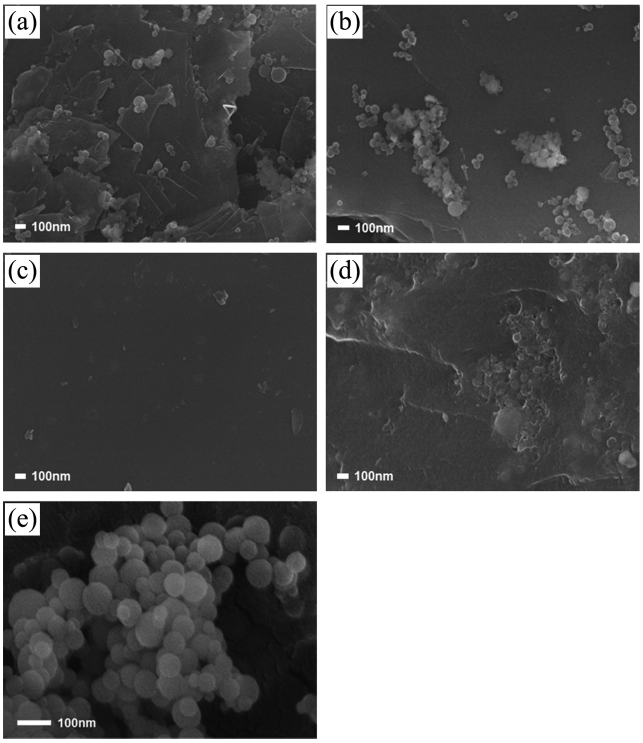

Figure 3. SEM images of Si/C composites and Si nanopowder: (a) Si-GB; (b) Si-PCB; (c) SiE-SC; (d) SiE-HC; and (e) as-received Si nanoparticles.

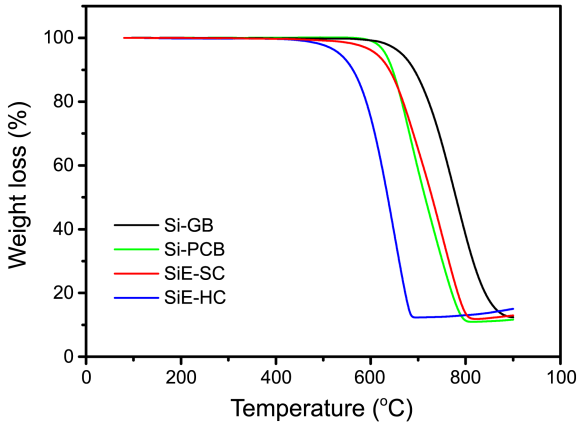

Figure 4. TGA curves of Si/C composites.

The temperature range where rapid weight loss due to the oxidation of carbon occurred was observed to depend strongly on the carbon type (Fig. 4). The oxidation of graphite in Si-GB terminated at much higher temperature (near 900 °C) than the other composites. After the weight loss reached a maximum, a more gradual increase in the sample weight was observed, possibly caused by the oxidation of silicon powder (Fig. 4). The silicon content was determined from the maximum weight loss due to carbon oxidation. The amounts of silicon in Si-GB, Si-PCB, SiE-SC and SiE-HC were 12.4, 10.9, 11.8 and 12.3 wt %, respectively.

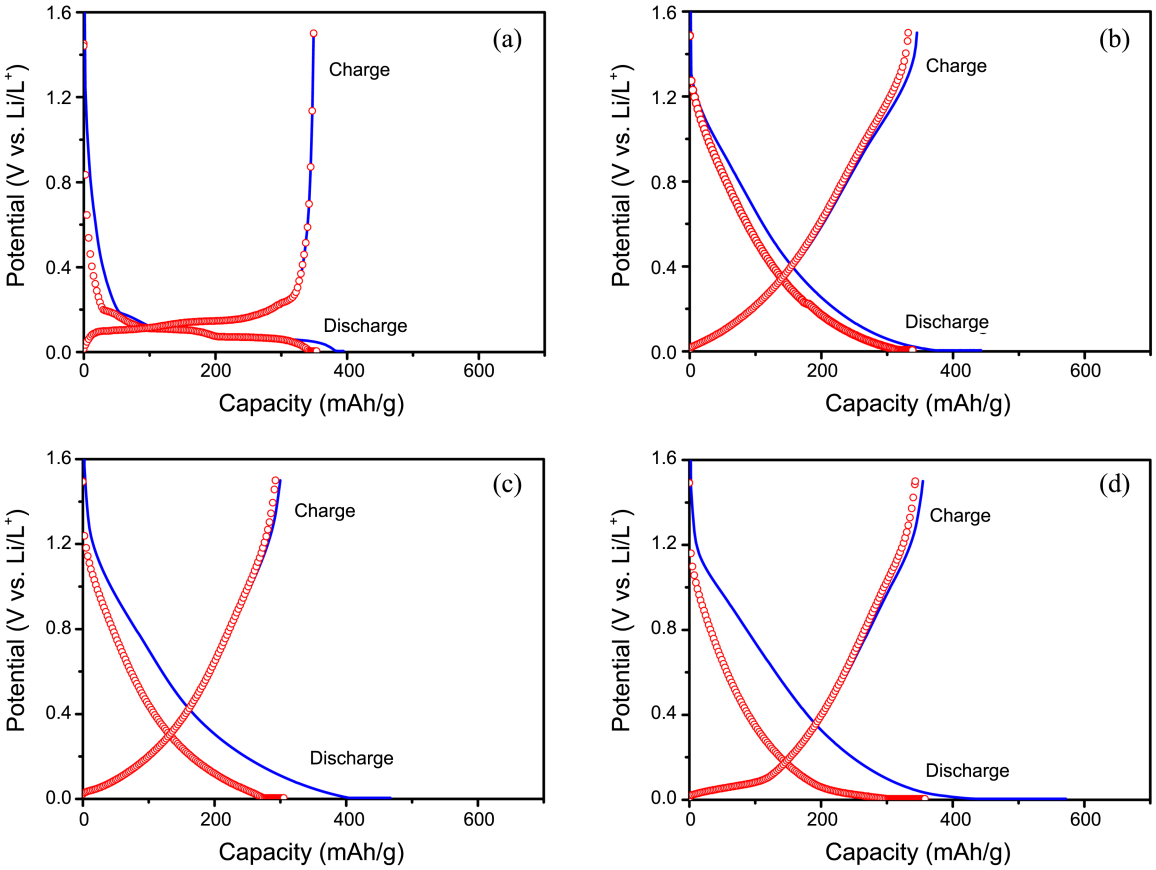

Figure 5. First (–) and second (○) charge/discharge curves of the pure carbons: (a) graphite; (b) petroleum coke-based carbon; (c) pitch-based carbon; and (d) sucrose-based carbon.

Table 1. Results for the four carbon materials during the first two cycles of the charge/discharge tests

Samples	Capacity (mAh/g)				Coulombic efficiency (%)	
	1st cycle		2nd cycle			
	Discharge	Charge	Discharge	Charge	1st cycle	2nd cycle
Graphite (MCMB)	394	349	354	349	88.6	98.6
Coke-based carbon	442	345	338	332	78.1	98.2
Pitch-based carbon	467	300	305	292	64.2	95.7
Scurose-based carbon	572	354	358	343	61.9	95.8

Table 2. Results for the four Si/C composites during the first two cycles of the charge/discharge tests

Samples	Capacity (mAh/g)				Coulombic efficiency (%)	
	1st cycle		2nd cycle			
	Discharge	Charge	Discharge	Charge	1st cycle	2nd cycle
Si-GB	817	586	569	538	71.7	94.6
Si-PCB	780	553	535	490	70.9	91.6
SiE-SC	887	670	663	640	75.5	96.5
SiE-HC	864	639	625	594	74.0	95.0

Figure 5 shows the charge (lithium deinsertion)/discharge (lithium insertion) curves of the four carbon materials during the first two cycles. The graphite and the two disordered carbons (prepared from petroleum coke and sucrose) showed higher charge capacities (approximately 350 mAh/g in the first cycle) than pitch-based carbon (300 mAh/g). Unlike graphite, a large amount of lithium was extracted from the three disordered carbons in the high potential range between 0.4 and 1.5 V during charging, which is typically observed in carbon materials prepared at low temperatures.[22] Table 1 summarizes the results of the charge/discharge tests for the carbon samples. After the formation of the solid electrolyte

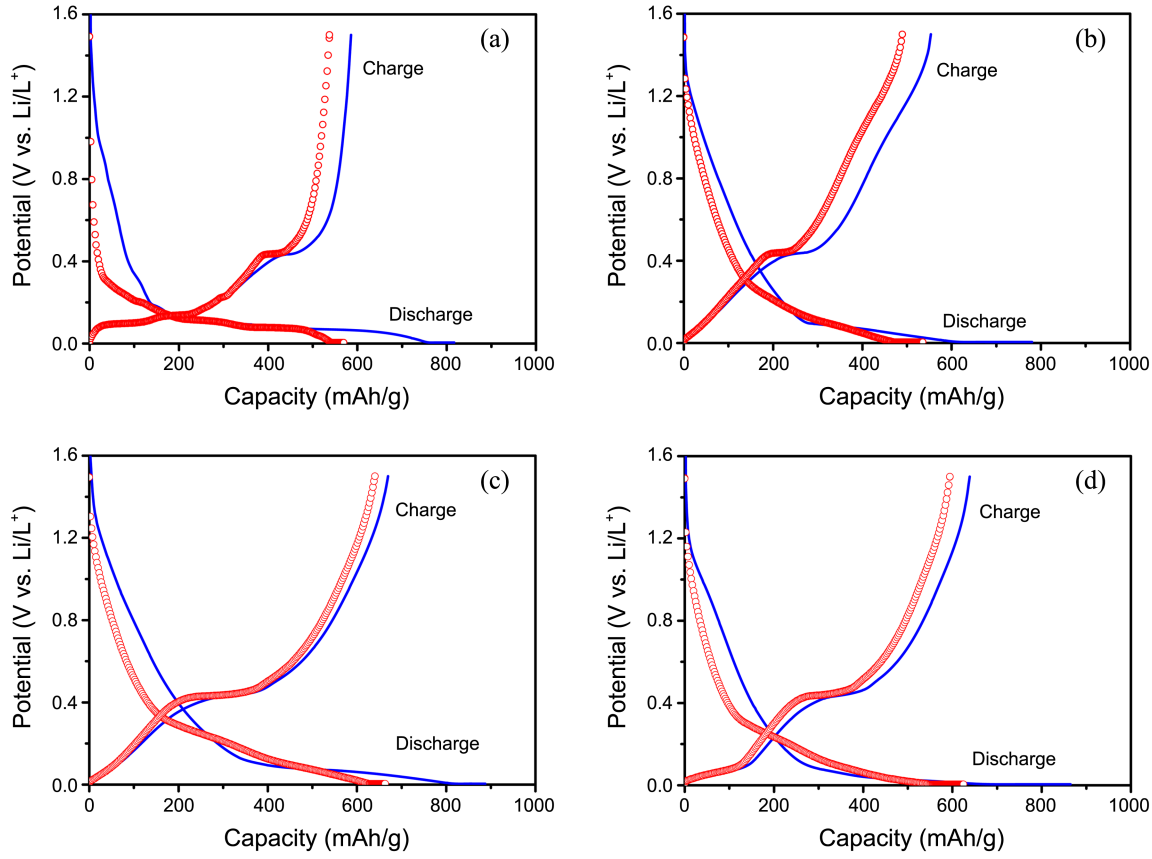

Figure 6. First (–) and second (○) charge/discharge curves of the Si/C composites: (a) Si-GB; (b) Si-PCB; (c) SiE-SC; and (d) SiE-HC.

Table 3. Summary of Si content, contribution of Si to the discharge capacities of the composites and specific capacities of Si of the four Si/C composite materials in the first cycle

Samples	Si Content[a] (%)	$Q_{expected}$[b] (mAh/g-composite)	$Q_{measured}$[c] (mAh/g-composite)	Utilization of Si[d] (%)	Specific Capacity of Si[e] (mAh/g-Si)
Si-GB	12.4	444	280	63.2	2260
Si-PCB	10.9	390	246	63.0	2253
SiE-SC	11.8	422	405	96.0	3436
SiE-HC	12.3	440	329	74.6	2671

[a]Silicon content of the Si/C composites determined by TGA. [b]Capacity of the Si nanoparticles, which was calculated based on the Si content and the theoretical specific capacity of Si (3579 mAh/g) at room temperature [23]. [c]Capacity was determined by subtracting the charge capacity of Si/C composites from that of the carbon materials in the first cycle. [d]Silicon utilization percent was calculated by dividing the $Q_{measured}$ by the $Q_{expected}$. [e]Specific capacity of Si was estimated from the utilization of Si and the theoretical specific capacity of Si (3579 mAh/g) at room temperature [23].

interface (SEI) layers on the carbon surface during the first discharge, the four carbon materials showed very high coulombic efficiency, over 95%, since the second cycle.

The four Si/C composite samples showed significantly higher charge capacities (> 550 mAh/g) in the first cycle due to the contribution of the silicon particles (Fig. 6). The alloying/dealloying process of the Si-Li alloys occurred below approximately 0.4 V *vs*. Li/Li^+. To estimate the utilization of Si in the Si/C composites during charge/discharge, the capacities expected for Si nanoparticles ($Q_{expected}$) in the four Si/C materials were calculated based on the Si content and the theoretical capacity of Si (3579 mAh/g) (Table 3).[23] In addition, experimental capacities of the Si nanoparticles ($Q_{measured}$) were determined by subtracting the charge capacities of the Si/C composites from those of the corresponding carbon materials in the first cycle, assuming that the carbon matrices fully participate in the charge/discharge process. The percent silicon utilization was calculated by dividing $Q_{measured}$ by $Q_{expected}$ (Table 3). Surprisingly, the SiE-SC exhibited very high Si utilization (96.0%), indicating that most of the Si particles were electrically well connected to the carbon matrix. Si-GB, Si-PCB and SiE-HC also presented good Si utilization (~63 to ~75%), although these values are relatively low when compared with SiE-SC.

In the Si/C samples, the coulombic efficiencies ($Q_{charge}/Q_{discharge}$) of the first and second cycles were above 70 and 90%, respectively (Table 2). Interestingly, the coulombic efficiencies were higher for the silicon-embedded samples (SiE-SC and SiE-HC) than the corresponding carbon materials during the first cycle, whereas the opposite trend was observed for the silicon-blended samples (Si-GB and Si-PCB) (Tables 1 and 2). This behavior may be caused by the high coulombic efficiency of the embedded Si particles in the carbon matrices, where the Si particles are not exposed to the electrolytes. This result is consistent with SEM observations (Fig. 3). The cycling behavior of the pure carbon samples was examined to identify the characteristics of the carbon matrices before the cycle performance tests of the Si/C composite samples. Graphite showed the best cycle retention, 99% over 40 cycles. In addition, the disordered carbons based on pitch, coke and sucrose carbon precursors showed good cycle retention of 93, 92, 86%, respectively, although their capacity gradually diminished over 40 cycles (Fig. 7(a)). In contrast, the silicon-blended samples (Si-GB

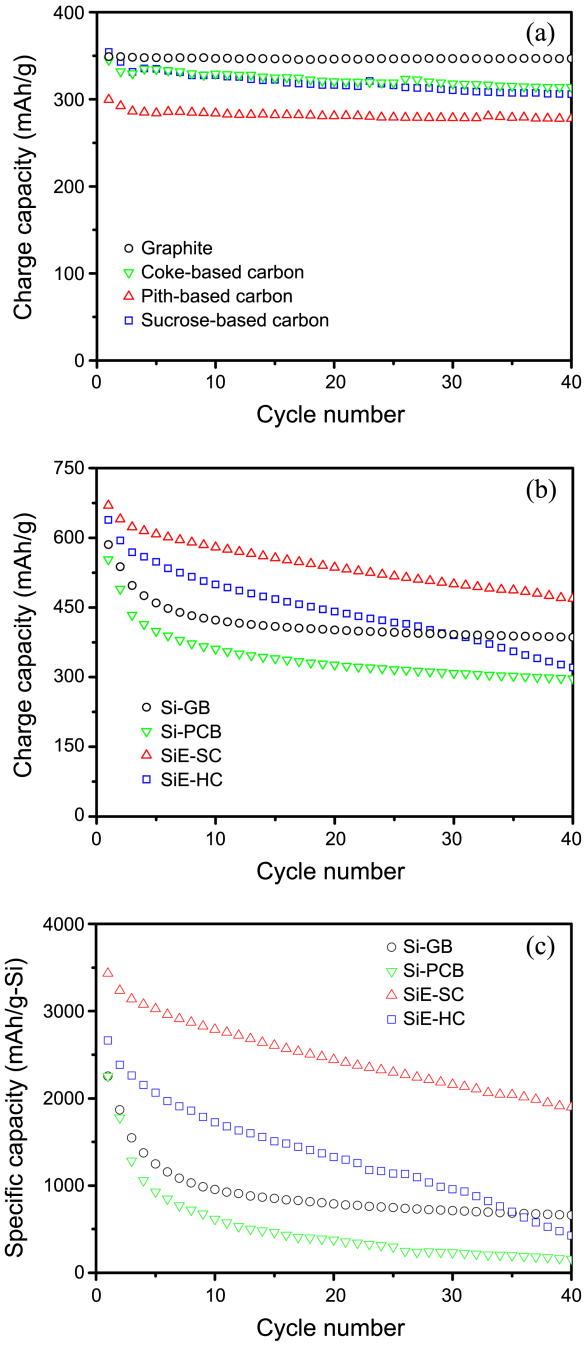

Figure 7. Cycle properties of the pure carbons (a), Si/C composites (b) and Si particles (c) in Si/C composites.

and Si-PCB) and SiE-HC showed a very rapid decrease in capacity during the first 10 cycles (Fig. 7(b)). The SiE-SC composite exhibited excellent cycle performance and maintained its charge capacity of 470 mAh/g during 40 cycles. We suppose that the big difference in cycle performance between SiE-HC and SiE-SC may be caused by the degree of dispersion of Si nanoparticles within carbon matrix. It seems that the large volume expansion/contraction of Si particles in SiE-HC was not effectively accommodated by the carbon matrix due to the poor dispersion of Si nanoparticles, resulting in poor cycle performance. The contributions of Si to the cycle performance of the Si/C composites were analyzed using the cycle data for the carbon and Si/C samples (Figs. 7(a) and 7(b)). The specific capacities of Si were calculated from the Si utilization and $Q_{measured}$ for each cycle. The Si nanoparticles in the SiE-SC exhibited high specific capacities of about 1900 mAh/g after 40 cycles, which correspond to 55% of their initial capacities (Fig. 7(c)). In contrast, the other Si/C composites retained only 7, 16 and 29% of their original capacities. The overall results imply that the Si nanoparticles in the SiE-SC composite were thoroughly encapsulated, and the volume expansion/contraction of Si would be effectively accommodated by the surrounding carbons matrix that was derived from pitch.

Conclusion

Four types of Si/C composites were prepared from graphite, petroleum coke, pitch and sucrose carbon precursors. A ball mill was used to prepare Si/C blends from graphite and petroleum coke, whereas a dispersion technique was used to prepare composites where Si was embedded in pitch or sucrose. SEM observations confirmed that the Si nanoparticles were well dispersed on the surface of the carbon matrix in Si-GB and Si-PCB, whereas the Si nanoparticles were encapsulated by the carbon matrix in SiE-SC and SiE-HC. The electrochemical performance of the pure carbon materials and the Si/C composites was analyzed carefully, and utilization and cycle behaviors of the Si particles in the Si/C composites were estimated. SiE-SC exhibited extremely high Si utilization (96% in the first cycle) and 70% capacity retention after 40 cycles. The best cycle performance was obtained for Si particles in SiE-SC. We concluded that the Si nanoparticles in the SiE-SC sample were encapsulated, and the volume change of the Si nanoparticles will be accommodated by the carbon matrix derived from pitch in battery applications, when compared with scurose-based carbon matrix. We expect that the cycle performance of the SiE-SC will be enhanced greatly when electrodes are constructed from a proper binder system or when cells are assembled with an optimized electrolyte system.

Acknowledgments. This study was supported by the Basic Science Research Program (NRF, 2012-0002775) and the Education and Research Promotion Program of KOREATECH.

References

1. Tarascon, J.-M.; Armand, M. *Nature* **2001**, *414*, 359.
2. Bruce, P. G.; Scrosati, B.; Tarascon, J.-M. *Angew. Chem. Int. Ed.* **2008**, *47*, 2.
3. Poizot, P.; Laruelle, S.; Grugeon, S.; Dupont, L.; Tarascon, J.-M. *Nature* **2000**, *407*, 496.
4. Idota, Y.; Kubota, T.; Matsufuji, A.; Maekawk, Y.; Miyasaka, T. *Science* **1997**, *276*, 1395.
5. Yu, Y.; Chen, C.-H.; Shi, Y. *Adv. Mater.* **2007**, *19*, 993.
6. Ng, S.-H.; Wang, J.; Wexler, D.; Konstantinov, K.; Guo, Z.-P.; Liu, H.-K. *Angew. Chem. Int. Ed.* **2006**, *45*, 6896.
7. Yang, X.; Zhang, P.; Wen, Z.; Zhang, L. *J. Alloys Compd.* **2010**, *496*, 403.
8. Zuo, P.; Yin, G.; Yang, Z.; Wang, Z.; Cheng, X.; Jia, D.; Du, C. *Mater. Chem. Phys.* **2009**, *115*, 757.
9. Gu, P.; Cai, R.; Zhou, Y.; Shao, Z. *Electrochim. Acta* **2010**, *55*, 3876.
10. Wen, Z. S.; Yang, J.; Wang, B. F.; Wang, K.; Liu, Y. *Electrochem. Commun.* **2003**, *5*, 165.
11. Ahn, D.; Raj, R. *J. Power Sources* **2011**, *196*, 2179.
12. Luo, Z.; Fan, D.; Liu, X.; Mao, H.; Yao, C.; Deng, Z. *J. Power Sources* **2009**, *189*, 16.
13. Guo, Z. P.; Milin, E.; Wang, J. Z.; Chen, J.; Liu, H. K. *J. Electrochem. Soc.* **2005**, *152*, A2211.
14. Si, Q.; Hanai, K.; Imanishi, N.; Kubo, M.; Hirano, A.; Takeda, Y.; Yamamoto, O. *J. Power Sources* **2009**, *189*, 761.
15. Guo, Z. P.; Jia, D. Z.; Yuan, L.; Liu, H. K. *J. Power Sources* **2006**, *159*, 332.
16. Kim, I.-S.; Kumta, P. N. *J. Power Sources* **2004**, *136*, 145.
17. Lee, J.-H.; Kim, W.-J.; Kim, J.-Y.; Lim, S.-H.; Lee, S.-M. *J. Power Sources* **2008**, *176*, 353.
18. Yang, J. B.; Wang, F.; Wang, K.; Liu, Y.; Xie, J. Y.; Wen, Z. S. *Electrochem. Solid-State Lett.* **2003**, *6*, A154.
19. Zuo, P.; Yin, G.; Ma, Y. *Electrochim. Acta* **2007**, *52*, 4878.
20. Hwang, S. S.; Cho, C. G.; Kim, H. *Electrochim. Acta* **2010**, *55*, 3236.
21. Jung, Y.; Suh, M. C.; Lee, H.; Kim, M.; Lee, S.-I. S.; Shim, C.; Kwak, J. *J. Electrochem. Soc.* **1997**, *144*, 4280.
22. Zheng, T.; Xue, J. S.; Dahn, J. R. *Chem. Mater.* **1996**, *8*, 389.
23. Obrovac, M. N.; Christensen, L. *Electrochem. Solid State Lett.* **2004**, *7*, A93.